NATURAL SCIENCE RESEARCH LABORATORY
TEXAS TECH

Occasional Papers

Museum at Texas Tech University Number 394 16 July 2026

Revisiting Subfossil Small-eared Shrews of the Genus *Cryptotis* Pomel, 1848 from Near Copán, Honduras, with the Description of a New Species (Mammalia: Eulipotyphla: Soricidae)

Neal Woodman and Darin A. Croft

Abstract

In 2005, we reported on the skeletal remains of shrews (Mammalia: Eulipotyphla: Soricidae) in an assemblage of small mammals excavated in 1941–1942 from an unknown cave north of Copán, Honduras. The identified elements comprised three species that we identified as *Cryptotis goodwini* Jackson, 1933, *C. merriami* Choate, 1970, and *C. orophilus* (Allen, 1895). The remains of *C. goodwini* were remarkable because, based on the sizes of the dentary and humerus, they represented an animal 39–52% lower in mass than modern members of the species, and we hypothesized the remains were from a Pleistocene population that underwent size increase early in the Holocene. Since 2005, *C. goodwini* has undergone extensive taxonomic revision, and the name is now understood to have been applied to a complex of at least 13 closely related sky island species, with nominal *C. goodwini* (*sensu stricto*) restricted to south central Guatemala. The new taxonomic paradigm prompted us to re-examine the excavated shrew remains from near Copán and further investigate their context. We can now more precisely identify the collection site as the cavern known to archaeologists as Gordon's Cave #3, which was documented as having an extensive late Holocene bone deposit. Our review of the shrew remains indicates they represent a member of the *C. goodwini* clade, but a species smaller than any known member of that group. Herein, we describe this as a new, previously unrecognized, probably extant species from the highlands north of Copán.

Key words: body size, Central America, copanensis, diversification, McGrew's Cave, mountain, new species, sky island, threatened species

Introduction

During 1941–1942, Paul McGrew of the Field Museum (FMNH), Chicago, and Albert A. Potter of Nebraska State Teachers College, Chadron, excavated bone-rich sediments from an unidentified cave north of the Copán archaeological site, Copán Department, western Honduras (Fig. 1). Excavated materials from the site, which we referred to as "McGrew's Cave" (Woodman and Croft 2005), were stored in Guatemala until after the end of the Second World War, when they were shipped to the FMNH. Animal remains from the

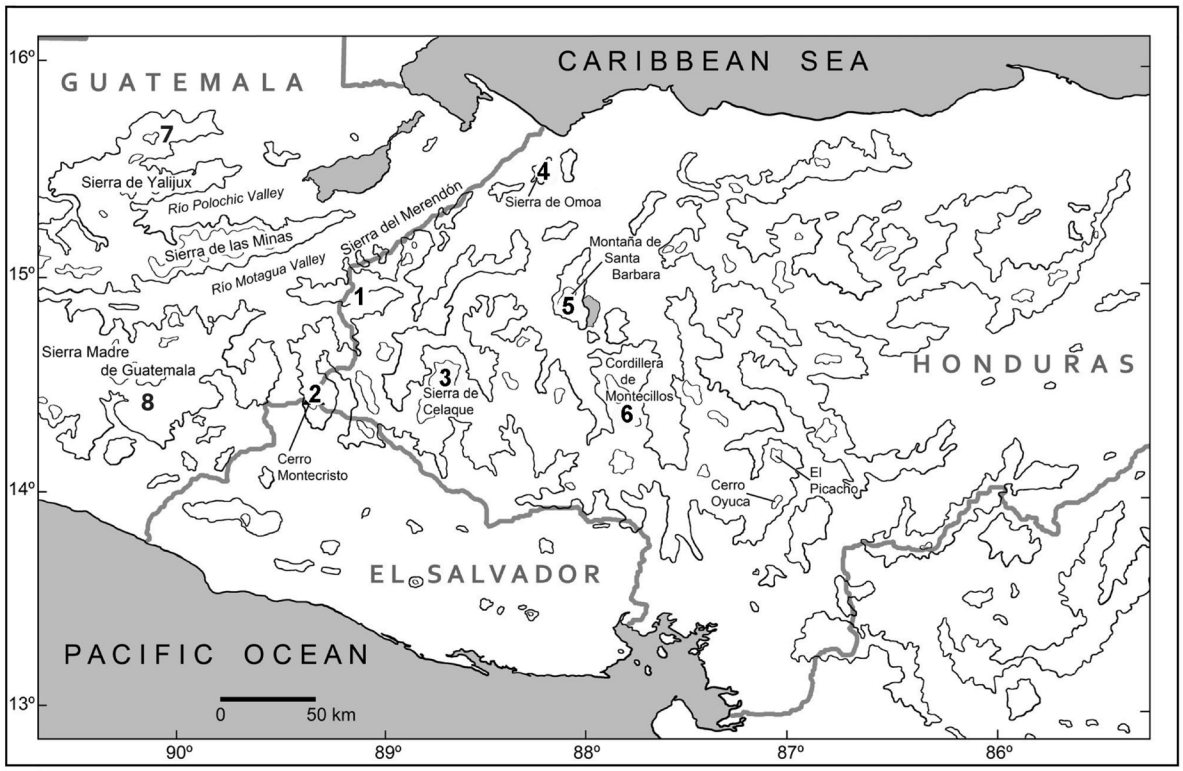

Figure 1. Map of eastern Guatemala and western Honduras showing the location of McGrew's Cave (a.k.a. Gordon's Cave #3) north of Copán and the known distributions of species of *Cryptotis goodwini* group shrews in this region. Honduras: 1) Gordon's Cave #3; 2) *C. montecristo*; 3) *C. celaque*; 4) *C. mccarthyi*; 5) *C. cavatorculus*; and 6) *C. magnimanus*. Guatemala: 7) *C. oreoryctes*; and 8) *C. matsoni*. Contour interval is 1,000 m.

cave remained mostly uncatalogued and unexamined until Croft (1998) studied them as part of a master's program at the University of Chicago. In addition to uncounted bones of avians, reptiles, and amphibians, he identified skeletal elements of at least 396 individuals of 29 taxa of small mammals, an aggregation whose composition was considered generally typical of a modern tropical highland fauna in western Honduras. The most common identifiable mammalian remains from the cave were those of small-eared shrews (Soricidae: *Cryptotis* Pomel, 1848), cotton rats (Cricetidae: *Sigmodon* Ord and Say, 1825), and harvest mice (Cricetidae: *Reithrodontomys* Giglioli, 1874). The shrews comprised three species that we subsequently identified as *Cryptotis goodwini* Jackson, 1933, *C. merriami* Choate, 1970, and *C. orophilus* (Allen, 1895) (Woodman and Croft 2005).

In 2005, *C. goodwini* was recognized as a widespread highland species with a geographical distribution extending from the southern Sierra Madre of Chiapas, Mexico, through the highlands of Guatemala into western Honduras (Woodman and Timm 1999). Skeletal remains of *C. goodwini* were relatively easy to distinguish from those of other shrews in the region based on their greater overall size and the distinctive morphologies of the skull and certain postcranial bones, particularly the humerus (Woodman and Timm 1999; Woodman 2005; Woodman and Croft 2005). *Cryptotis goodwini* is a member of a clade in which the fore limbs are modified to enhance digging ability. The humerus is robust and has enlarged processes, including a broad and elongate teres tubercle and expanded medial and lateral epicondyles (Woodman and Gaffney 2014; Guevara 2017). Remains identified as *C. goodwini* from McGrew's Cave were of particular interest because the dentaries averaged 10% shorter than those of modern *C. goodwini*, and mean length of the humerus was 4% shorter than that for modern *C. goodwini*. These size differences were interpreted as representing a popula-

tion of that species that was 6–24% shorter in head-and-body length and 39–52% lower in mass than modern members of the species (Woodman and Croft 2005).

Many mammals that survived the end-Pleistocene extinctions in North America experienced changes in body size during the climatic changes that marked the Pleistocene-Holocene transition (Lundelius et al. 1983; Woodman and Croft 2005:Table 8; Meachen and Samuels 2012). The pattern of size change suggested that those species whose modern representatives exhibit a Bergmann's response (i.e., body size increases with latitude) had greater body size in the Late Pleistocene and decreased in body size into the Holocene. In contrast, species that exhibit a reverse Bergmann's response (body size decreases with latitude) increased in size during the transition to the Holocene (Lundelius et al. 1983). Although the majority of mammals display a Bergmann's response (Millien et al. 2006), most soricids display a reverse Bergmann's response (Ochocińska and Taylor 2003; Yom-Tov and Yom-Tov 2005).

In addition to the small *C. goodwini* recovered from McGrew's Cave, two excavated dentaries of a rice rat (Cricetidae: *Oryzomys* Baird, 1857) and two dentaries from the big-eared climbing rat (Cricetidae: *Ototylomys phyllotis* Merriam, 1901) represented individuals that would have been larger than any members of their respective modern species known from the region. The size differences in these three species relative to their modern representatives suggested a possible Late Pleistocene age for at least some of the fauna. Unfortunately, bone from the cave yielded insufficient carbon to obtain radiometric dates. Fecal pellets presumed to be from rodents or bats presented a modern date of 10 ± 40 yr BP (TX-9344) and charcoal from the sediments yielded a late Holocene date of 2940 ± 110 yr BP (TX-9345). The latter date was calibrated at one sigma with CALIB rev8.2 (Stuiver and Reimer 1993) to ca. 3206–3053–2880 cal BP (1257–1104–931 cal BC). These dates and the differences in sizes of skeletal elements led to an interpretation of a mostly Holocene fauna possibly mixed with Late Pleistocene elements (Woodman 2005; Woodman and Croft 2005).

Subsequent to the publication of our original work, additional collections of Central American small mammals have become available for study (Woodman et al. 2012; Ordóñez-Garza et al. 2014; Matson et al. 2015), and the taxonomy and systematics of Central American small-eared shrews has undergone considerable revision (Woodman 2018). In particular, *C. goodwini sensu lato* was shown to comprise a complex of at least 13 species, and the modern sample used for comparison with the excavated elements from McGrew's Cave included individuals that now are recognized as belonging to five Guatemalan and Mexican species, including: *C. goodwini* (*sensu stricto*), now restricted to the western Sierra Madre of Guatemala; *C. lacertosus* Woodman, 2010, endemic to the Sierra de los Cuchumatanes, Guatemala; *C. matsoni* Woodman, 2019, known only from isolated highlands in Jalapa Department, Guatemala; *C. oreoryctes* Woodman, 2011, endemic to the Sierra de Yalijux, Guatemala; and *C. woodmani* Guevara, 2023, endemic to the Sierra Madre de Chiapas, Mexico. Additional Honduran species allied to *C. goodwini* and previously identified as that species include *C. cavatorculus* Woodman, 2015, which occurs in the Montaña de Santa Barbara, Santa Barbara Department; *C. celaque* Woodman, 2015, endemic to the Sierra de Celaque, Lempira Department; *C. magnimanus* Woodman and Timm, 1999 in the Cordillera de Montecillos, Comayagua Department; *C. mccarthyi* Woodman, 2015 from the Sierra de Omoa, Cortés Department; and *C. montecristo* Woodman, 2019, endemic to Cerro Montecristo, a highland at the convergence of the borders of El Salvador, Guatemala, and Honduras (Fig. 1). Based on dentary length, the sample identified as "*C. goodwini*" from McGrew's Cave represents a shrew that averaged smaller than any of these species (Fig. 2).

The purpose of this paper is to re-evaluate the remains excavated from McGrew's Cave previously identified as *C. goodwini* in the context of the current taxonomy of small-eared shrews. We provide additional details regarding the identity, location, and history of the cave from which the remains were excavated. We also revise our interpretation of possible Late Pleistocene to Holocene size change in *C. goodwini* by recognizing the remains as representing a new, probably extant species of small-eared shrew that we describe herein.

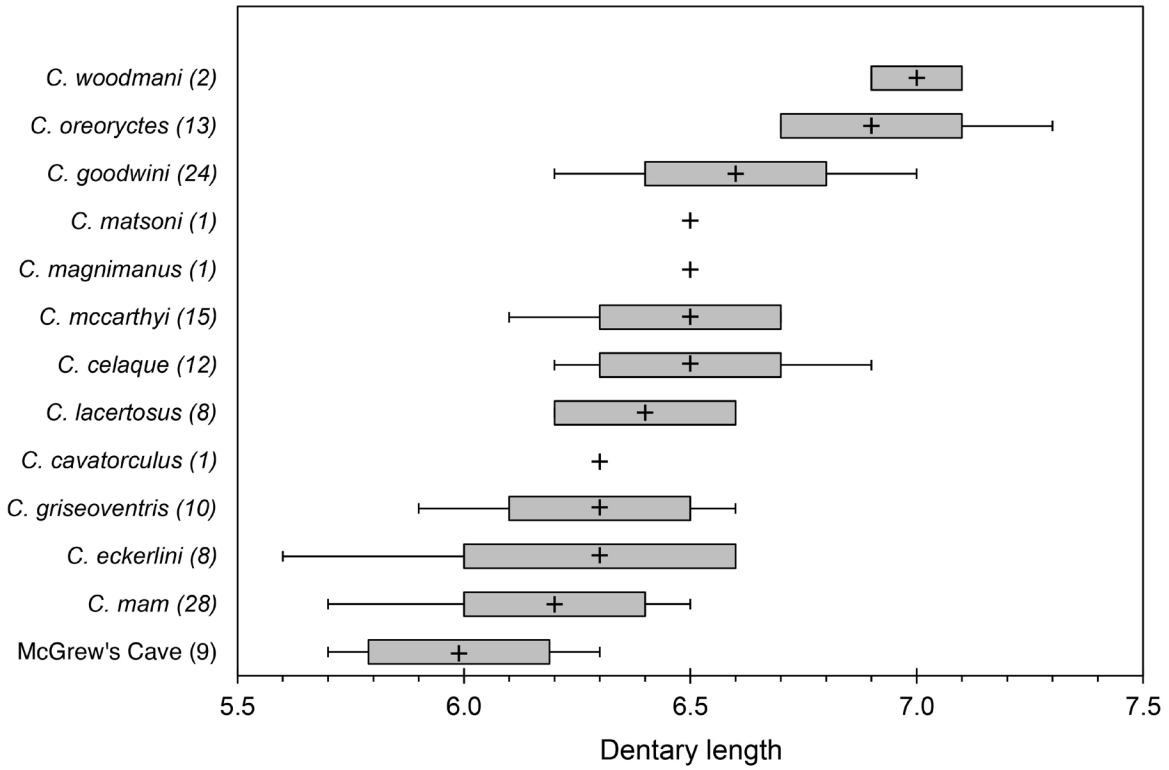

Figure 2. Box-and-whisker plot showing relative sizes (in mm) among species of the *C. goodwini*-group as measured by dentary length (DL). The dentaries from McGrew's Cave (a.k.a. Gordon's Cave #3) are noticeably shorter than those of any other species in the group. Statistics represented are the sample mean (cross) ± one standard deviation (gray box) and range (vertical lines). Sample size for each species is provided in parentheses.

STUDY SITE

McGrew and Potter's excavation of the cave north of the Copán archaeological site was a minor part of a larger expedition, the primary objective of which was to collect fossils from Honduras that would help clarify the timing of the emergence of the Panamanian land corridor between Central and South America and address other issues related to the mixing of mammal faunas from the two regions during what now is called the Great American Biotic Interchange (Stehli and Webb 1985). After three months quarrying Pliocene deposits in the Department of Gracias (Olson and McGrew 1941; McGrew 1942, 1944), much of the remainder of the expedition was spent excavating Pleistocene large mammals in Yeroconte Quarry, Copán Department. Although details of these activities were described in McGrew's field notes archived in the Field Museum of Natural History, the excavation of sediments in the cave north of Copán was never mentioned. The only record of this collection consists of a few sentences written by McGrew on a 5" x 7" index card that states:

> These specimens are part of a great quantity taken from a cave roughly five miles north of Copan, Honduras. The top two feet of debris in the third room of the cave was made up almost entirely of bone. There is a considerable quantity of this material waiting shipment with our other things from Guatemala City. McGrew

Whether the material now at the Field Museum comprises the entire collection from the cave is unknown.

The exact location of the cave McGrew and Potter visited was unspecified. Few caves are present north of Copán, however, and the short description of "the top two feet of debris in the third room of the cave" is consistent with only one of them: a multi-chambered cavern initially explored and described by the archaeologist George Byron Gordon (1898) that archaeologists have subsequently referred to as Gordon's Cave #3 (Rue et al. 1989; Brady 1995, 1996). We hereafter use that name to refer to the cave we previously called "McGrew's Cave."

Gordon (1898:139) located the cave "about four miles from the principal group of ruins, towards the northwest, in a limestone ridge that rises abruptly from the rocky bed of a mountain stream called the Sesesmil." This cave "consists of three chambers, of which the first or outer is the largest. Just inside the entrance was an old abandoned eagle's nest surrounded by heaps of bones of small animals, such as squirrels, small hog, tepisquintli [*Cuniculus paca* (Linnaeus, 1766)], young deer, and many other species" (Gordon 1898:141). In the third chamber of the cave, Gordon (1898:143) noted "a mass of charred and calcined bones occupied the entire floor to a depth of about two feet." Later excavations in the third chamber by Rue et al. (1989) confirmed a 40-cm-thick layer of human remains that were estimated to represent 600–700 individuals. The site was interpreted as either a Mayan ossuary or a location for agricultural rites during the Middle Preclassic (ca. 1000–400 BC) to Late Classic (ca. 600–900 AD) periods, with its heaviest use during the latter period (Brady 1995). These activities potentially spanned the period of 2950–1050 yr BP, which is not inconsistent with the calibrated radiocarbon date of 3206–3053–2880 cal BP on charcoal from the sediments that we reported previously (Woodman and Croft 2005). The presence of human remains in the material obtained by McGrew and Potter (Croft 1998; Woodman and Croft 2005) is also consistent with their excavation of the third chamber of Gordon's Cave #3.

Rue et al. (1989) and Brady (1995) more precisely located Gordon's Cave #3 in a limestone ridge (ca. 14°51'45" N, 89°10'20" W) on the east side of Quebrada Sesesmil near its headwaters, approximately 3 km due north of Copán. Both Rue et al. (1989) and Brady (1995, 1996) provided maps of the cave chambers. The variation in distances of the cave from Copán archaeological site as reported by McGrew's index card, Gordon (1898), Rue et al. (1989), and Brady (1995) probably reflects differences between straight-line and road distances and how those distances were estimated.

Portions of Gordon's Cave #3, including part of the third chamber, were excavated by several different archaeological parties whose primary interest was in cultural and human remains. In excavations carried out in 1896 and 1897, Gordon (1898) reached estimated depths of 15 ft (4.6 m) in chamber 1, 6 ft (1.8 m) in chamber 2, and 3 ft (0.9 m) in chamber 3. Richard MacNeish excavated a test pit in chamber 2 in 1957 in search of early evidence of maize agriculture (Rue et al. 1989; Brady 1995). In 1983, two 180-cm-deep test pits were dug in chamber 1 and three 70-cm-deep test pits in chamber 3 by David J. Rue and AnnCorinne Freter (Rue et al. 1989). Brady (1995, 1996) excavated the upper 70 cm of sediments in four test pits in chamber 1 in 1991. Gordon (1898:11), Rue et al. et al. (1989:398), and Brady (1995:35) all noted the presence of large numbers of small mammal bones in the cave sediments. Gordon (1898:11) considered the non-human bones to be "generally rodents," whereas Rue et al. (1989:398) called them "primarily bat" remains. Notwithstanding Gordon's (1898) observation of an abandoned raptor nest in the first chamber of the cave, he and Brady (1995, 1996) suggested that the presence of non-human bones, some of which were burned, was primarily the result of human activity in the form of offerings or sacrifices. Unfortunately, there is no evidence that any of the archaeological studies attempted more precise identifications of the non-human remains, and none produced a substantive taxonomic list of the excavated fauna.

MATERIALS AND METHODS

Our re-examination of specimens from Gordon's Cave #3 previously identified as *C. goodwini* (*sensu lato*) relied on data obtained from three left and nine right dentaries and nine left and six right humeri. These specimens were compared with modern specimens of all known species of the *C. goodwini* group from

Honduras and two species from eastern Guatemala. Comparative samples included *C. cavatorculus* (*n* = 1 dentary, 1 humerus), *C. celaque* (*n* = 12 dentaries, 3 humeri), *C. magnimanus* (*n* = 1 dentary, 1 humerus), *C. matsoni* (*n* = 1 dentary, 1 humerus), *C. mccarthyi* (*n* = 15 dentaries, 1 humerus), *C. montecristo* (*n* = 1 dentary), and *C. oreoryctes* (*n* = 8 dentaries, 5 humeri). Specimens examined are listed in the Appendix. The small sample sizes for the comparative samples reflect the limited availability of specimens in systematic collections. *Cryptotis cavatorculus*, *C. magnimanus*, and *C. matsoni*, for example, are still known only from their holotypes (but see Beck et al. 2024). Specimens from the following institutions were examined (Appendix; abbreviations follow Dunnum et al. 2018:SD4): Carnegie Museum of Natural History, Pittsburgh (CM); Colección Nacional de Mamíferos, Instituto de Biología, Universidad Nacional Autónoma de México, México City (CNMA); Florida Museum of Natural History, Gainesville (FLMNH); Field Museum of Natural History, Chicago (FMNH); University of Kansas Natural History Museum and Biodiversity Institute, Lawrence (KU); Museum of Comparative Zoology, Cambridge (MCZ); The Natural History Museum, London (NHM); Senckenberg Naturmuseum, Frankfurt (SMF); Museum at Texas Tech University, Lubbock (TTU); Museum of Zoology, University of Michigan, Ann Arbor (UMMZ); Universidad Nacional Autónoma de Honduras, Tegucigalpa (UNAH); Museo de Historia Natural, Universidad de San Carlos de Guatemala, Guatemala City (USAC); National Museum of Natural History, Washington (USNM); and Museum Köenig, Bonn (ZMFK).

Tooth homologies follow Hutterer (2005), who specified a dental formula for *Cryptotis* of I1, I2, I3, C, P1, P4, M1, M2, M3 / i1, i2, p4, m1, m2, m3. Dental terminology follows Choate (1970), and features of the dentary are shown in Figure 3 (see also Woodman and Timm 1992, 1993, 1999; Woodman and Croft 2005: Fig. 2). Postcranial terminology follows Reed (1951), and features of the humerus are shown in Figure 4 (see also Woodman and Timm 1999; Woodman and Croft 2005:Fig. 3; Woodman and Gaffney 2014:Fig. 1). All measurements are in millimeters, and all masses are in grams. Dentary measurements (Table 1) follow Woodman and Timm (1993) and Woodman and Croft (2005: Fig. 4) and include: length of dentary (DL), measured from the lower sigmoid notch to the posterior edge of the mental foramen; height of coronoid process (HCP), from its base to its superior tip; height of coronoid valley (HCV), from the base of coronoid process to the upper sigmoid notch; height of articular condyle (HAC), from the base of coronoid process to the superior tip of articular condyle; superior tip of articular condyle to posterior edge of m3 (AC3); occlusal length of toothrow (TRD), from anterior edge of i2 to posterior edge of m3; length of lower molar row (M13), from anterior edge of m1 to posterior edge of m3; greatest length of m1 (M1L); and breadth of articular condyle (BAC), from the superior tip to the medio-inferior tip. Humerus measurements (Table 2) follow Woodman and Stabile (2015) and Woodman and Wilken (2019), and include: length of humerus, from the head to the trochlea (HL); length of the axis of rotation from the head to the trochlea/capitulum notch (HAR); distal width (epicondylar breadth) of humerus (HDW); length of deltopectoral crest (HDPC); least mediolateral diameter of humerus (HLD); distance from the head of the humerus to the distal edge of the teres tubercle (HTT); and length of the teres tubercle (HTTR). Variables were recorded to the nearest 0.1 mm using an ocular micrometer in a binocular microscope. Univariate statistics were calculated in Excel 97-2003 (Microsoft Corp., Redmond, Washington) and multivariate statistics in PAST 4.03 (Hammer et al. 2001). Relative characters and indices calculated from measurements are expressed as percentages. Tabular summary statistics include mean ± SD and range.

In the Diagnosis and Description, a measured character from a sample is described as "very short" or "very low" if its mean is ≥ 1 SD below the mean for the genus; "short" or "low" if its mean is ≥ ½ SD below the genus mean; "moderate" if within ± ½ SD of the genus mean; "large," "long," or "high" if ≥ ½ SD greater than the genus mean; or "very large," "very long," or "very high" if ≥ 1 SD greater than the genus mean. The mean for the genus is based on measurements from up to 60 species and distinctive populations of the genus *Cryptotis*.

To further examine the morphometrical distinctiveness of *Cryptotis* remains from Gordon's Cave #3 relative to other species in the region, we performed principal components analysis (PCA) and discriminant function analysis (DFA) on a correlation matrix of six $\log_{10}$-transformed dentary variables (DL, HCP, HCV,

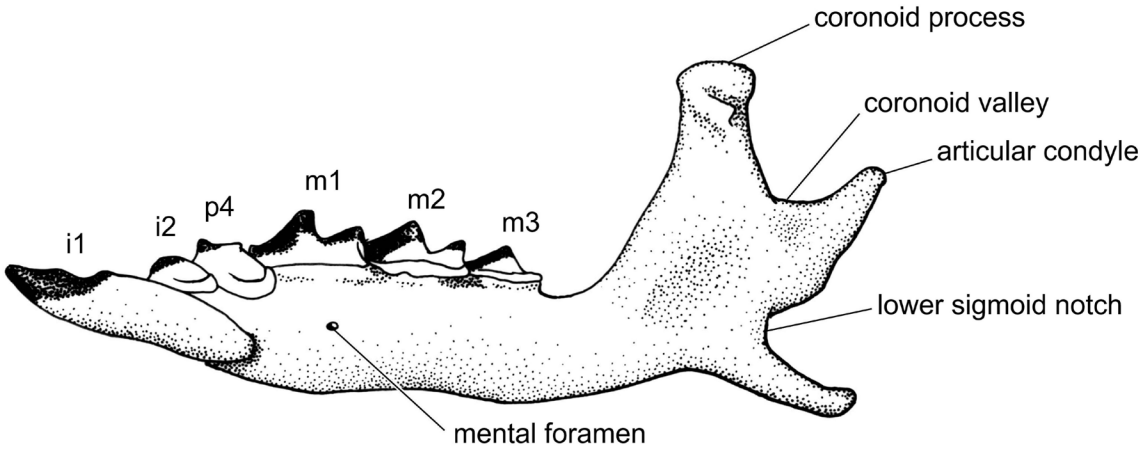

Figure 3. Lateral aspect of the left dentary of *Cryptotis* illustrating anatomic features and positions of the teeth.

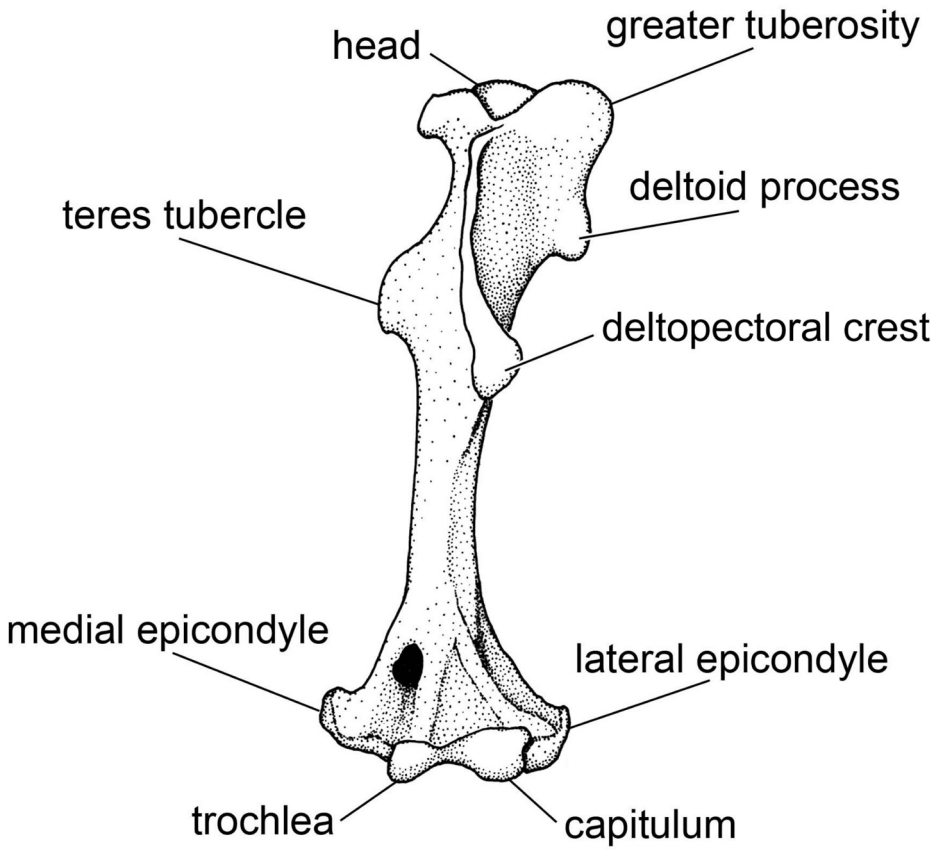

Figure 4. Anterior aspect of the left humerus of *Cryptotis nigrescens* illustrating anatomical features.

Table 1. Dentary measurements and indices of *C. copanensis* and seven other species of the *C. goodwini* group from Honduras and western Guatemala. Summary statistics are mean ± SD and range.

Cryptotis copanensis (left) (*n* = 3)	*Cryptotis copanensis* (right) (*n* = 9)	*Cryptotis cavatorculus* (*n* = 1)	*Cryptotis celaque* (*n* = 12)	*Cryptotis magnimanus* (*n* = 1)	*Cryptotis matsoni* (*n* = 1)	*Cryptotis mccarthyi* (*n* = 15)	*Cryptotis montecristo* (*n* = 1)	*Cryptotis oreoryctes* (*n* = 14)
			MEASUREMENTS					
Length of dentary (DL)								
6.0 ± 0.1 5.9–6.1	6.0 ± 0.2 5.6–6.3 (*n* = 8)	6.3	6.5 ± 0.2 6.2–6.9	6.5	6.5	6.5 ± 0.2 6.1–6.7	—	6.9 ± 0.2 6.7–7.3
Height of coronoid process (HCP)								
4.5 ± 0.3 4.3–4.8	4.6 ± 0.1 4.4–4.7	4.6	4.7 ± 0.2 4.4–4.9	4.7	4.7	4.6 ± 0.2 4.3–4.9	4.8	4.8 ± 0.1 4.6–4.9
Height of articular valley (HCV)								
2.7 ± 0.2 2.5–2.9	2.8 ± 0.1 2.6–3.0	2.8	2.9 ± 0.1 2.6–3.0	2.9	3.0	2.8 ± 0.1 2.7–3.1	2.8	3.1 ± 0.1 3.0–3.2
Height of articular condyle (HAC)								
3.6 ± 0.1 3.5–3.7	3.8 ± 0.1 3.6–4.0	3.8	4.0 ± 0.2 3.5–4.2	4.1	4.1	3.9 ± 0.2 3.6–4.2	4.1	4.2 ± 0.1 3.9–4.3
Posterior length of dentary (AC3)								
4.6 (*n* = 1)	4.8 ± 0.1 4.7–5.1 (*n* = 5)	5.0	5.2 ± 0.2 4.9–5.3	5.3	5.3	5.1 ± 0.2 4.8–5.4	5.6	5.6 ± 0.2 5.1–6.0
Length of lower toothrow (TRD)								
—	5.8, 5.9 (*n* = 2)	6.2	6.4 ± 0.2 6.1–6.6	5.9	6.2	6.2 ± 0.2 5.9–6.4	6.5	6.5 ± 0.2 6.1–6.8
Length of lower molar row (M13)								
4.5 (*n* = 1)	4.4 ± 0.1 4.4–4.6 (*n* = 5)	4.4	4.6 ± 0.1 4.5–4.8	4.4	4.6	4.6 ± 0.1 4.3–4.8	4.8	4.8 ± 0.2 4.5–5.0

Table 1. (cont.)

Cryptotis copanensis (left) ($n = 3$)	*Cryptotis copanensis* (right) ($n = 9$)	*Cryptotis cavatorculus* ($n = 1$)	*Cryptotis celaque* ($n = 12$)	*Cryptotis magnimanus* ($n = 1$)	*Cryptotis matsoni* ($n = 1$)	*Cryptotis mccarthyi* ($n = 15$)	*Cryptotis montecristo* ($n = 1$)	*Cryptotis oreoryctes* ($n = 14$)
Length of first lower molar (M1L)								
1.7, 1.8 ($n = 2$)	1.8 ± 0.05 1.7–1.8 ($n = 8$)	1.8	1.8 ± 0.1 1.7–1.9	1.8	1.9	1.8 ± 0.04 1.7–1.8	2.0	1.8 ± 0.1 1.7–1.9
Breadth of articular condyle (BAC)								
2.8 ± 0.04 2.7–2.8 ($n = 3$)	2.9 ± 0.1 2.8–3.0	3.1	3.0 ± 0.1 2.8–3.2	3.1	3.2	3.0 ± 0.1 2.9–3.2	3.3	3.2 ± 0.1 3.0–3.4 ($n = 8$)
			INDICES					
($n = 3$)	($n = 8$)	($n = 1$)	($n = 12$)	($n = 1$)	($n = 1$)	($n = 15$)	($n = 1$)	($n = 14$)
HCP/DL								
74.6 ± 4.4 71.0–79.4	74.6 ± 4.4 71.0–79.4	74.1	72.0 ± 2.3 68.4–75.4	72.3	72.3	71.3 ± 3.3 66.8–79.3	—	69.8 ± 2.2 66.7–73.7
BAC/DL								
45.8 ± 0.2 45.6–46.0	48.7 ± 2.0 46.3–51.6	50.0	46.2 ± 2.1 42.7–49.0	47.7	49.2	47.2 ± 1.6 44.5–50.7	—	47.1 ± 2.1 43.8–50.1 ($n = 8$)
AC3/DL								
77.6 ($n = 1$)	82.0 ± 3.6 76.5–84.8 ($n = 5$)	79.7	79.5 ± 2.5 75.1–83.6	81.5	81.5	78.9 ± 2.9 75.0–83.5	—	81.8 ± 2.7 76.1–85.6
AC3/HCP								
105.7 ($n = 1$)	106.1 ± 1.1 104.1–107.0 ($n = 5$)	107.5	110.3 ± 3.1 105.3–117.4	112.8	112.8	110.7 ± 3.0 104.5–116.4	116.7	117.3 ± 3.8 110.9–125.8

Table 2. Humerus measurements and indices from *C. copanensis* and six other species of the *C. goodwini* group from Honduras and western Guatemala. Summary statistics are mean ± SD and range.

Cryptotis copanensis (left) (n = 3)	*Cryptotis copanensis* (right) (n = 2)	*Cryptotis cavatorculus* (n = 1)	*Cryptotis celaque* (n = 3)	*Cryptotis magnimanus* (n = 1)	*Cryptotis matsoni* (n = 1)	*Cryptotis mccarthyi* (n = 1)	*Cryptotis oreoryctes* (n = 5)
			MEASUREMENTS				
Humerus length (HL)							
7.90 ± 0.07 7.82–7.94	7.82, 8.00	8.35	7.89 ± 0.18 7.69–8.01	8.27	8.14	8.04	8.29 ± 0.31 7.85–8.69
Axis of rotation length (HAR)							
7.40 ± 0.17 7.21–7.52	7.33, 7.57	7.88	7.38 ± 0.12 7.24–7.47	7.86	7.59	7.55	7.78 ± 0.27 7.39–8.11
Distal width (HDW)							
4.00, 4.12 (n = 2)	3.99 (n = 1)	4.34	3.99 ± 0.15 3.82–4.13	4.50	4.28	4.08	4.46 ± 0.33 4.12–5.00
Deltopectoral crest length (HDPC)							
4.11 ± 0.11 4.03–4.24	4.00, 4.24	4.18	3.54 ± 0.08 3.49–3.63	3.55	3.38	3.48	3.66 ± 0.17 3.45–3.89
Least diameter (HLD)							
0.99 ± 0.08 0.90–1.03	1.03, 1.03	1.04	0.99 ± 0.04 0.95–1.01	1.07	1.02	1.04	1.11 ± 0.07 0.99–1.17
Head to teres tubercle (HTT)							
3.76 ± 0.10 3.70–3.88	3.64, 3.91	3.79	3.61 ± 0.11 3.50–3.71	3.92	3.84	3.45	3.96 ± 0.20 3.70–4.17
Teres tubercle length (HTTR)							
2.08 ± 0.14 1.94–2.21	1.93, 2.06	2.50	2.29 ± 0.11 2.17–2.38	2.32	2.40	2.25	2.63 ± 0.16 2.42–2.78
			INDICES				
(n = 4)	(n = 2)	(n = 1)	(n = 3)	(n = 1)	(n = 1)	(n = 1)	(n = 5)
HDW/HL							
51.6 ± 0.6 51.2–52.0 (n = 2)	49.9 (n = 1)	52.0	50.5 ±0.9 49.7–51.5	54.4	52.6	50.7	53.8 ±2.1 52.3–57.5
HDPC/HL							
52.2 ± 1.1 51.1–53.5	51.2, 53.0	50.1	44.9 ± 0.9 43.9–45.4	42.9	41.5	43.2	44.1 ± 1.4 42.8–46.3

Table 2. (cont.)

Cryptotis copanensis (left) (n = 3)	*Cryptotis copanensis* (right) (n = 2)	*Cryptotis cavatorculus* (n = 1)	*Cryptotis celaque* (n = 3)	*Cryptotis magnimanus* (n = 1)	*Cryptotis matsoni* (n = 1)	*Cryptotis mccarthyi* (n = 1)	*Cryptotis oreoryctes* (n = 5)
HLD/HL							
12.6 ± 0.7 11.5–13.0	12.9, 13.2	12.5	12.6 ± 0.7 11.9–13.2	12.9	12.5	13.0	13.4 ± 0.6 12.6–14.0
HTTR/HL							
26.1 ± 1.3 24.8–27.8	24.7, 25.8	29.9	29.0 ± 1.9 27.1–31.0	28.1	29.5	28.0	31.8 ± 2.9 28.6–35.4
HAR/HL							
93.7 ± 1.4 92.2–94.7 (n = 3)	93.7, 94.6	94.4	93.5 ± 0.6 93.0–94.2	95.0	93.2	93.9	93.9 ± 0.6 93.2–94.6
HTT/HL							
47.5 ± 0.9 46.7–48.9	46.5, 48.9	45.4	45.8 ± 2.2 43.9–48.2	47.4	47.2	42.9	47.8 ± 1.5 45.8–49.6

HAP, M1L, BAC). This combination of variables permitted the inclusion of eight right and two left dentaries from Gordon's Cave #3. Analyses compared the excavated dentaries with those from *C. cavatorculus*, *C. celaque*, *C. magnimanus*, *C. matsoni*, *C. mccarthyi*, and *C. oreoryctes*. *Cryptotis montecristo* was not included in these analyses because the dentaries of the holotype are incomplete (Woodman 2019). This last species was found to be distinctive, however, in being much larger in most other dentary measurements than the Gordon's Cave #3 dentaries (Table 1; Fig. 5).

We also carried out PCA on a correlation matrix of six $\log_{10}$-transformed humerus variables (HL, HDPC, HLD, HTTR, HAR, HTT). This analysis included three left and two right humeri from Gordon's Cave #3, which were compared with humeri from one *C. cavatorculus*, three *C. celaque*, one *C. magnimanus*, one *C. matsoni*, one *C. mccarthyi*, and five *C. oreoryctes*. *Cryptotis montecristo* was not included in these analyses because the humerus is not known. Specimens from the cave included in multivariate analyses are listed in bold type in the following description.

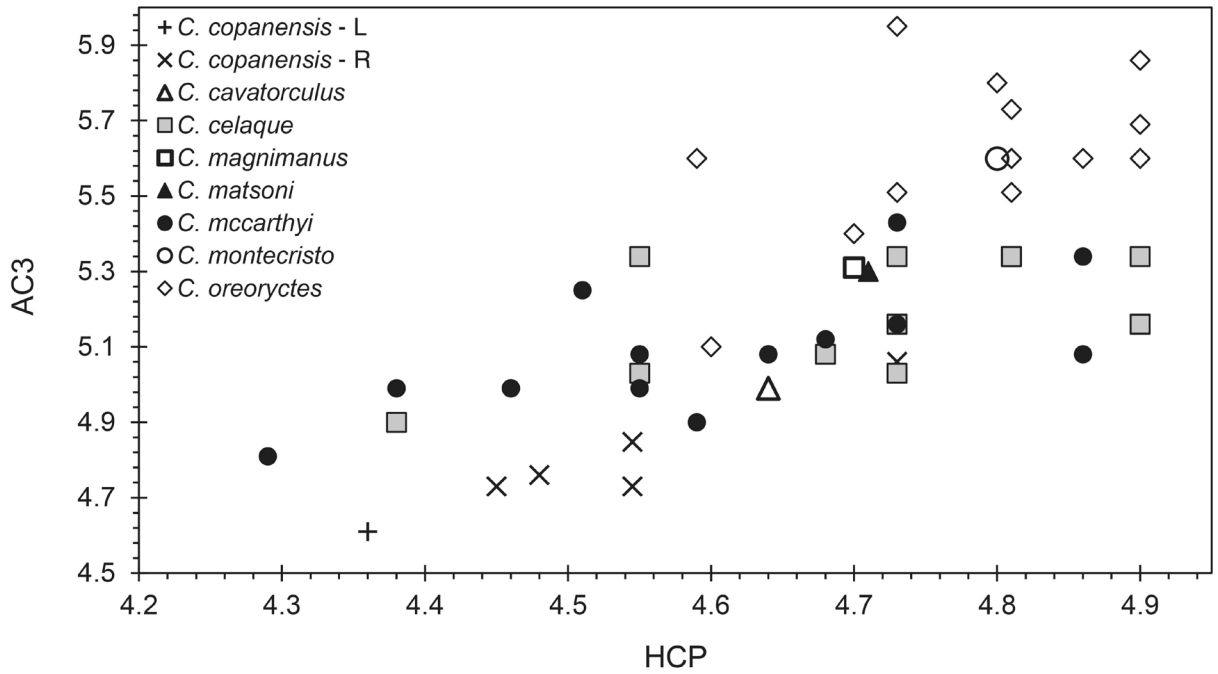

Figure 5. Plot of posterior length of the dentary (AC3) versus height of the coronoid process (HCP), illustrating that *C. copanensis* is generally smaller than seven other species of large-footed *Cryptotis* from Honduras and western Guatemala. Because of the possibility that left (L) and right (R) dentaries of *C. copanensis* originated from the same individual, they are separated in this graph.

SYSTEMATIC ZOOLOGY

Genus *Cryptotis* Pomel, 1848

Small-eared or Least Shrews

Cryptotis goodwini group

Molecular phylogenetic analyses have shown that the northern Central American broad-clawed shrews of the *Cryptotis goodwini* group (Clade VI of He et al. 2021) represent a clade that is separate from, but possibly closely related to, Mexican broad-clawed shrews of the *Cryptotis goldmani* group (Clade III of He et al. 2021), which includes the three species *C. alticola* (Merriam, 1895), *C. goldmani* (Merriam, 1895), and *C. peregrinus* (Merriam, 1895) (Baird et al. 2017; Moreno Cárdenas 2017; He et al. 2021; Mejía-Fontecha et al. 2021; Cifuentes 2026). Previously, members of the *C. goodwini* group were considered part of the *C. goldmani* group (Woodman and Timm 1999).

Cryptotis copanensis sp. nov.

Copán Broad-clawed Shrew

(Figs. 6, 7)

Synonymy.—*Cryptotis goodwini*: Woodman and Croft, 2005 (part).

Holotype.—Right dentary of an adult of unknown sex, Field Museum of Natural History, Department of Geology, FMNH-PM 17098; excavated 1941–1942 by Paul McGrew and Albert A. Potter. The dentary is complete with all teeth present (i1, i2, p4, m1, m2, m3).

Type locality.—Honduras: Copán Department; third chamber of Gordon's Cave #3, approximately 3 km north of Copán (approximately 14°51'45" N, 89°10'20" W).

Paratypes.—Left dentaries (3): FMNH-PM 17065, **17138**, **17154**. Right dentaries (9): FMNH-PM 17053, **17068**, **17071**, **17075**, **17081**, **17083**, **17098**, **17100**, **57551**. Left humeri (9): FMNH-PM 59423, 59424, 59425, 59426, 59427, 59428, **59429**, **59430**, **59431**. Right humeri (6): FMNH-PM 59380, 59381, 59382, 59383, **59384**, **59385**.

Distribution.—Known only from the type locality in Honduras. The species probably occurs in moist highland forests ≥ 1,000 mamsl north of Copán.

Etymology.—The specific epithet refers to the archaeological site of Copán, Copán Department, Honduras, near where the type material was obtained.

Nomenclatural statement.—The Life Sciences Identifier (LSID) number for *Cryptotis copanensis* is urn:lsid:zoobank.org:pub:B4B4CAFC-D390-46B3-BE8A-4CE696F7B05A.

Diagnosis.—Based on the morphology of the dentary and humerus, *Cryptotis copanensis* is a broad-clawed shrew in the *C. goodwini* group (clade VI of He et al. 2021). The dentary can be distinguished morphologically from those of most other species in the genus by the combination of its high coronoid process, the anterior border of which joins the horizontal ramus at a relatively low angle; posterior border of the i1 cingulum is generally anterior to the posterior border of p4 and aligned anteroposteriorly with the posterior border of the paraconid of m1; long posterior portion of mandible (articular process to posterior border of m3); relatively tall, wide articular process; deep lower sigmoid notch; relatively long, low-crowned i2; entoconid lacking from the talonid of m3 (See Woodman and Timm 1992, 1993, 1999). The massive humerus is relatively short and broad with a dorso-ventrally elongate head; a long, broad teres tubercle positioned more distally (rather than more proximally) along the shaft; wide medial and lateral epicondyles forming a broad distal edge; and a pronounced deltoid process (see Woodman and Gaffney 2014: Fig. 1). External and cranial morphology currently are unknown, but based on other members of the *C. goodwini* group, *C. copanensis* should have a very short to moderately long tail (averaging 30–41% of head and body length), broad fore feet, and long, broad fore claws (see Woodman and Timm 1999:Figs. 16, 17).

Cryptotis copanensis can be distinguished from the two other species of small-eared shrews identified from Gordon's Cave #3, *C. orophilus* (*C. parvus* group; Clade I of He et al., 2021) and *C. merriami* (*C. nigrescens* group; Clade VII of He et al. 2021), in having the anterior border of the coronoid process joining the horizontal ramus at a relatively low angle; lower sigmoid notch deep rather than shallow (*C. orophilus*) or absent (*C. merriami*); posterior edge of i1 cingulum anterior to posterior border of p4 and not extending posteriorly beyond that paraconid of m1; relatively higher and narrower articular process; and long, low-crowed i2. The humerus of *C. copanensis* is much larger and more robust with much larger processes and a larger teres tubercle located more distally along its shaft (Woodman and Croft 2005).

Cryptotis copanensis can be distinguished from the seven other Honduran and eastern Guatemalan species in the *C. goodwini* group by the smaller overall sizes of its dentary and humerus (Figs. 2, 7; Tables 1, 2). It has a short dentary (absolutely shorter than *C. cavatorculus*, *C. celaque*, *C. magnimanus*, *C. matsoni*, *C. mccarthyi*, *C. oreoryctes*); moderately high coronoid process (absolutely shorter than *C. oreoryctes*, *C. montecristo*; averages shorter than *C. celaque*, *C. magnimanus*, *C. matsoni*); moderately high coronoid valley (absolutely shorter than *C. oreoryctes*; averages shorter than *C. celaque*, *C. matsoni*); shorter articular condyle of the dentary (absolutely shorter than *C. magnimanus*, *C. matsoni*, *C. montecristo*, *C. oreoryctes*; averages shorter than *C. celaque*, *C. mccarthyi*); shorter posterior dentary as measured by AC3 (absolutely shorter than in all seven other species); shorter lower toothrow, i2–m3 (absolutely shorter than in *C. cavatorculus*, *C. celaque*, *C. matsoni*, *C. mccarthyi*, *C. montecristo*, *C. oreoryctes*; averages shorter than *C. magnimanus*) and shorter lower molar-row, m1–m3 (absolutely shorter than *C. montecristo*, *C. oreoryctes*; averages shorter than *C. celaque*, *C. matsoni*, *C. mccarthyi*); moderately long m1 (absolutely shorter than *C. matsoni*, *C. montecristo*; averages shorter than *C. oreoryctes*); narrower articular condyle (absolutely narrower than *C. cavatorculus*, *C. magnimanus*, *C. matsoni*, *C. mccarthyi*, *C. montecristo*, *C. oreoryctes*; averages narrower than *C. celaque*).

Cryptotis copanensis has a short humerus (absolutely shorter than in *C. cavatorculus*, *C. magnimanus*, *C. matsoni*, *C. mccarthyi*, *C. oreoryctes*) with a narrow

Figure 6. Lateral, dorsal, and lingual views of the right dentary of *C. copanensis* (FMNH-PM 59430—holotype). The scale bar is 5 mm in length.

Figure 7. Anterior (left) and posterior aspects of the left humerus of *C. copanensis* (FMNH-PM 59430). The scale bar is 5 mm in length.

distal width (absolutely narrower than in *C. cavatorculus*, *C. magnimanus*, *C. matsoni*, *C. oreoryctes*); a long deltopectoral crest (absolutely and relatively longer than in *C. celaque*, *C. magnimanus*, *C. matsoni*, *C. mccarthyi*, *C. oreoryctes*); narrow least diameter of the diaphysis (absolutely narrower than in *C. matsoni*, *C. oreoryctes*); and short teres tubercle (absolutely and relatively shorter than in *C. cavatorculus*, *C. celaque*, *C. magnimanus*, *C. matsoni*, *C. mccarthyi*, *C. oreoryctes*).

Description.—A small-eared shrew of the genus *Cryptotis* with a short dentary within the genus (Table 1; DL = 6.0 ± 0.2 vs. 6.4 ± 0.7 for the genus); the dentary has a coronoid process of medium height (HCP = 4.5 ± 0.1 vs. 4.6 ± 0.5 for the genus) that is nonetheless high relative to the length of the dentary (HCP/DL = 75.9% ± 3.5 vs. 71.3% ± 5.5 for the genus); the anterior border of the coronoid process joins the horizontal ramus of the mandible at a relatively low angle (see Woodman and Timm 1992, 1993, 1999); the posterior dentary, from the superior tip of the articular process to the posterior border of m3, is relatively long (AC3/DL = 81.3% ± 3.7 vs. 78.6% ± 5.8 for the genus); the articular condyle is moderately broad (BAC/DL = 47.9% ± 2.2 vs. 48.7% ± 2.1 for the genus); the inferior sigmoid notch is deep; the posterior border of the cingulum of i1 is generally anterior to posterior border of p4 and anteroposteriorly aligned with the posterior border of the paraconid of m1; i2 is proportionally long and low (see Woodman and Timm 1992, 1993, 1999); the entoconid is absent from the vestigial talonid of m3. The humerus is relatively short and broad with enlarged processes and a dorsoventrally elongate head (see Woodman and Gaffney 2014).

Comparisons

Cryptotis copanensis is distinguished from Honduran and eastern Guatemalan members of the *C. goodwini* group (*C. cavatorculus*, *C. celaque*, *C. magnimanus*, *C. matsoni*, *C. mccarthyi*, *C. montecristo*, *C. oreoryctes*) by its small size as indicated by its dentary, dentition, and humerus (Figs. 2, 5, 7; Tables 1, 2). The posterior dentary (AC3) of *C. copanensis* averages absolutely and relatively (AC3/HCP) shorter than in all seven other species (Fig. 5).

Cryptotis cavatorculus.—*Cryptotis copanensis* differs in averaging a shorter dentary (DL), shorter toothrow (TRD), and narrower articular condyle (BAC). The humerus is shorter (HL), narrower distally (HDW), and has an absolutely (HTTR) and relatively (HTTL/HL) shorter teres tubercle.

Cryptotis celaque.—*Cryptotis copanensis* differs in having a shorter dentary and lower toothrow (TRD). It averages a lower coronoid process (HCP), lower coronoid valley (HCV), shorter lower molar row (M13), and narrower articular condyle (BAC). Despite having an absolutely lower coronoid process, it is higher relative to dentary length (HCP/DL). The humerus has an absolutely (HTTR) and relatively (HTTL/HL) shorter teres tubercle that is positioned more distally along the diaphysis.

Cryptotis magnimanus.—*Cryptotis copanensis* differs in averaging a shorter dentary (DL) and lower coronoid process of the dentary (HCP) and having a lower (HAC) and narrower (BAC) articular condyle. Despite its absolutely lower coronoid process, this structure is higher relative to dentary length (HCP/DL). The humerus is shorter (HL) and narrower distally (HDW) and has an absolutely (HTTL) and relatively (HTTR/HL) shorter teres tubercle.

Cryptotis matsoni.—*Cryptotis copanensis* differs in averaging a shorter dentary (DL), lower coronoid process (HCP) and coronoid valley of the dentary (HCV), and shorter lower molar row (M13). It has a lower articular process (HAC); shorter lower toothrow (TRD); and shorter lower first molar (LM1). Despite its absolutely lower coronoid process, this structure averages higher relative to dentary length (HCP/DL). The humerus is shorter (HL), narrower distally (HDW), and has an absolutely (HTTL) and relatively (HTTR/HL) shorter teres tubercle (Fig. 7).

Cryptotis mccarthyi.—*Cryptotis copanensis* differs in having a shorter dentary (DL), lower toothrow (TRD), and narrower articular condyle (BAC). It averages a lower coronoid valley (HCV) and articular condyle (HAC) and shorter lower molar row (M13). It also averages a higher coronoid process relative to dentary length (HCP/DL). The humerus averages shorter (HL), has a narrower shaft diameter (HLD), and has an absolutely (HTTR) and relatively (HTTR/HL) shorter teres tubercle that is more proximally located along the shaft (HTT).

Cryptotis montecristo.—*Cryptotis copanensis* differs in averaging a shorter coronoid process (HCP), having a shorter lower toothrow (TRD) and lower molar row (M13), and a lower (HAC) and broader (BAC) articular condyle.

Cryptotis oreoryctes.—*Cryptotis copanensis* differs in having a shorter dentary (DL), lower toothrow (TRD), lower molar row (M13), and lower coronoid valley (HCV). Despite averaging a lower coronoid process (HCP), this structure averages higher relative to dentary length (HCP/DL). The humerus is shorter (HL) and narrower distally (HDW), has a narrower shaft diameter (HLD), and has an absolutely (HTTR) and relatively (HTTR/HL) shorter teres tubercle.

Results of Multivariate Analyses

Dentary analyses.—PCA of six $\log_{10}$-transformed dentary variables from *C. copanensis* and six other species of broad-clawed *Cryptotis* from Honduras and eastern Guatemala yielded a single principal component (PC1) with a significant eigenvalue based on a broken stick model (Jackson 1993), although broken stick values lie within the 95% confidence intervals for the second (PC2) and third (PC3) principal components based on 1000 bootstraps. All variables loaded positively on PC1, which accounted for more than 64% of the variance in the model and represented overall size of the dentary (Table 3). PC2, comprising nearly 14% of the variance, was mostly influenced by the length of the first lower molar (M1L), whereas PC3 was most strongly influenced by the length of the dentary (DL) and comprised more than 10% of the variance. In a plot of factor scores on PC1 and PC2 (not figured), all *C. copanensis* clustered in the left side of the plot, separate from *C. magnimanus*, *C. matsoni*, and *C. oreoryctes*, but intermixed with *C. cavatorculus* and smaller individuals of *C. celaque* and *C. mccarthyi*. In a plot of factor scores on PC1 and PC3 (Fig. 8), however, all *C. copanensis* were separated from the other six species in the lower left quadrant.

DFA of the same matrix of variables produced a correct classification rate of 71% among the seven species (Table 4). Although the correct classification rate was low overall, no *C. copanensis* was misclassified, and no individuals of other species were misidentified as *C. copanensis*. All misclassifications were individuals of *C. celaque*, *C. mccarthyi*, and *C. oreoryctes* identified as other species. The jackknifed classification was 54% correct. In that case, two *C. copanensis* were misclassified as *C. cavatorculus*, but no individuals of other species were misclassified as *C. copanensis*. The remaining misclassifications were among *C. celaque*, *C. matsoni*, *C. mccarthyi*, and *C. oreoryctes*.

Although there may be the potential for some confusion in multivariate space between the dentaries of *C. copanensis* and *C. cavatorculus*, the dentary of *C. copanensis* is more distinct morphologically than those of most other species in the region. Many more misidentifications occurred among *C. mccarthyi*, *C. celaque*, and *C. oreoryctes*, species that were initially identified morphologically and later corroborated by molecular analyses (He et al. 2015, 2021; Baird et al. 2017; Mejía-Fontecha 2021; Cifuentes 2026).

Humerus analyses.—PCA of six $\log_{10}$-transformed humerus variables from *C. copanensis* and six other species of broad-clawed *Cryptotis* from Honduras and eastern Guatemala yielded a single principal component (PC1) with a significant eigenvalue based on a broken stick model (Jackson 1993), although broken stick values lie well within the 95% confidence intervals for PC2. All variables except length of the deltopectoral crest (HDPC) loaded positively on PC1, which comprised nearly 62% of the variance in the model (Table 5). Despite the low loading of HDPC on PC1, this component was interpreted as generally representing overall size of the humerus. PC2, which constituted more than 22% of the variance, represented a contrast between HDPC, which loaded positively, and length of the teres tubercle (HTTR), which loaded negatively. In a plot of factor scores on the first two principal components (Fig. 9), all *C. copanensis* clustered in the upper left quadrant, separate from all other species, a result of the smaller overall size of the humerus and its relatively long deltopectoral crest and short teres tubercle.

Table 3. Component loadings and eigenvalues for the first three principal components (PCs) from a principal component analysis (PCA) of six $\log_{10}$-transformed dentary variables from *C. copanensis* and six other species of broad-clawed *Cryptotis* in the region (See Fig. 8). Variables are listed in descending order of their loadings on PC1. Variable abbreviations are explained in Materials and Methods and in Table 1.

Variable	PC1	PC2	PC3
HAP	0.461	-0.168	-0.136
HCV	0.452	-0.233	-0.263
HCP	0.444	-0.191	-0.290
BAC	0.437	-0.109	0.241
DL	0.358	0.229	0.813
M1L	0.259	0.904	-0.331
Eigenvalue	3.856	0.823	0.622
% variance	64.26	13.72	10.36

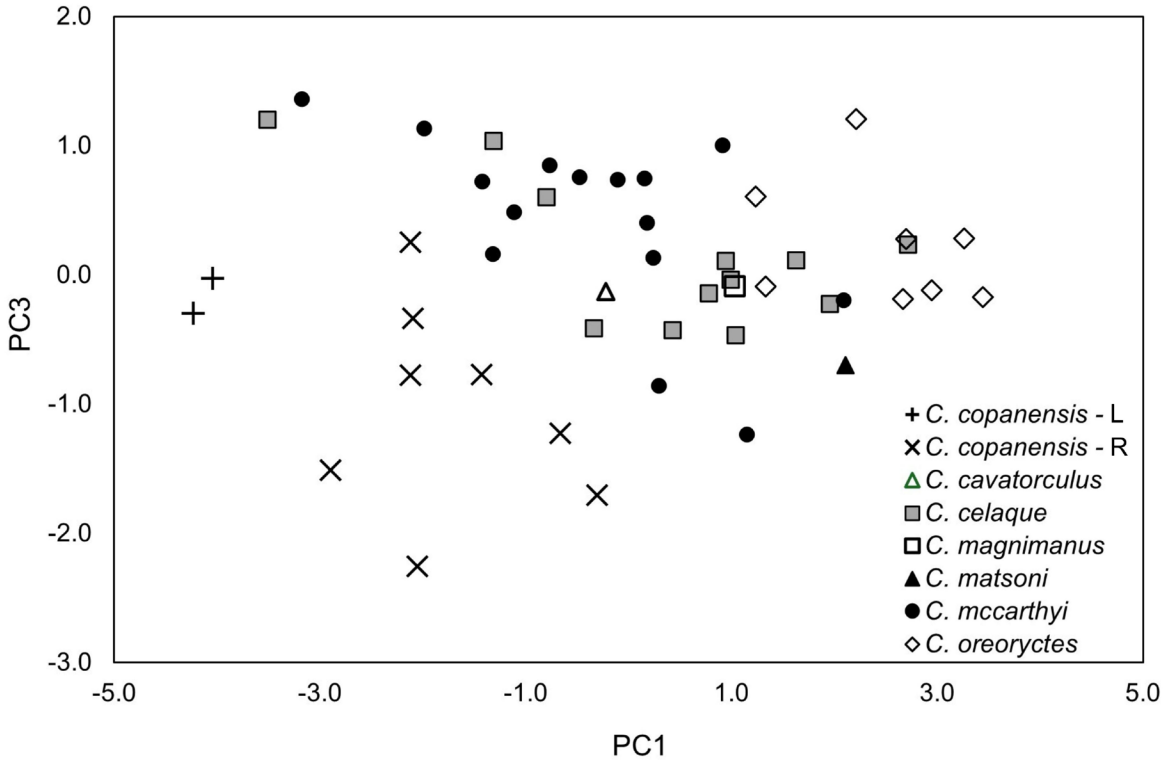

Figure 8. Plots of scores on first and third principal components from a PCA of six log10-transformed dentary variables from *C. copanensis* and six species of large-footed *Cryptotis* from Honduras and western Guatemala (see Table 3). Because of the possibility for left (L) and right (R) dentaries of *C. copanensis* to have come from the same individual, they are separated in this graph.

Table 4. Results of discriminant function analysis (DFA) of six log10-transformed dentary variables from *C. copanensis* and six other species in the region: a) Pearson correlations (loadings) of input variables on each canonical variate (CV). Variables are listed in descending order of their loadings on CV1; b) classification matrix; c) jackknifed classification matrix. Variable abbreviations are explained in Materials and Methods (Table 1).

a.

Variable	CV1	CV2	CV3
ML	69.420	38.644	5.887
HCV	45.200	-66.013	-3.225
BAC	33.190	-26.682	-61.066
HAP	7.716	20.159	24.400
M1L	-14.718	-65.171	42.816
HCP	-60.743	79.874	44.094
Eigenvalue	4.506	0.835	0.273
% variance	77.63	14.39	4.70

b.

	C. cop	*C. cav*	*C. cel*	*C. mag*	*C. mat*	*C. mcc*	*C. ore*	Total	% correct
C. copanensis	10	0	0	0	0	0	0	10	100
C. cavatorculus	0	1	0	0	0	0	0	1	100
C. celaque	0	2	5	3	0	2	0	12	42
C. magnimanus	0	0	0	1	0	0	0	1	100
C. matsoni	0	0	0	0	1	0	0	1	100
C. mccarthyi	0	2	1	2	0	10	0	15	67
C. oreoryctes	0	0	0	0	2	0	6	8	75
Total	10	5	6	6	3	12	6	48	71%

c.

	C. cop	*C. cav*	*C. cel*	*C. mag*	*C. mat*	*C. mcc*	*C. ore*	Total	% correct
C. copanensis	8	2	0	0	0	0	0	10	80
C. cavatorculus	0	1	0	0	0	0	0	1	100
C. celaque	0	2	4	4	0	2	0	12	33
C. magnimanus	0	0	0	1	0	0	0	1	100
C. matsoni	0	0	0	0	0	0	1	1	0
C. mccarthyi	0	2	3	4	0	6	0	15	40
C. oreoryctes	0	0	0	0	2	0	6	8	75
Total	8	7	7	9	2	8	7	48	54%

Table 5. Component loadings and eigenvalues for the first three principal components (PCs) from a principal component analysis (PCA) of six $\log_{10}$-transformed humerus variables from *C. copanensis* and six other species of broad-clawed *Cryptotis* in the region (see Fig. 9). Variables are listed in descending order of their loadings on the first factor axis. Variable abbreviations are explained in Materials and Methods and in Table 2.

Variable	PC1	PC2	PC3
HAR	0.493	0.094	-0.387
HL	0.473	0.064	-0.547
HLD	0.467	0.020	0.137
HTT	0.426	0.261	0.500
HTTR	0.364	-0.476	0.489
HDPC	-0.028	0.832	0.205
Eigenvalue	3.706	1.325	0.477
% variance	61.77	22.08	7.96

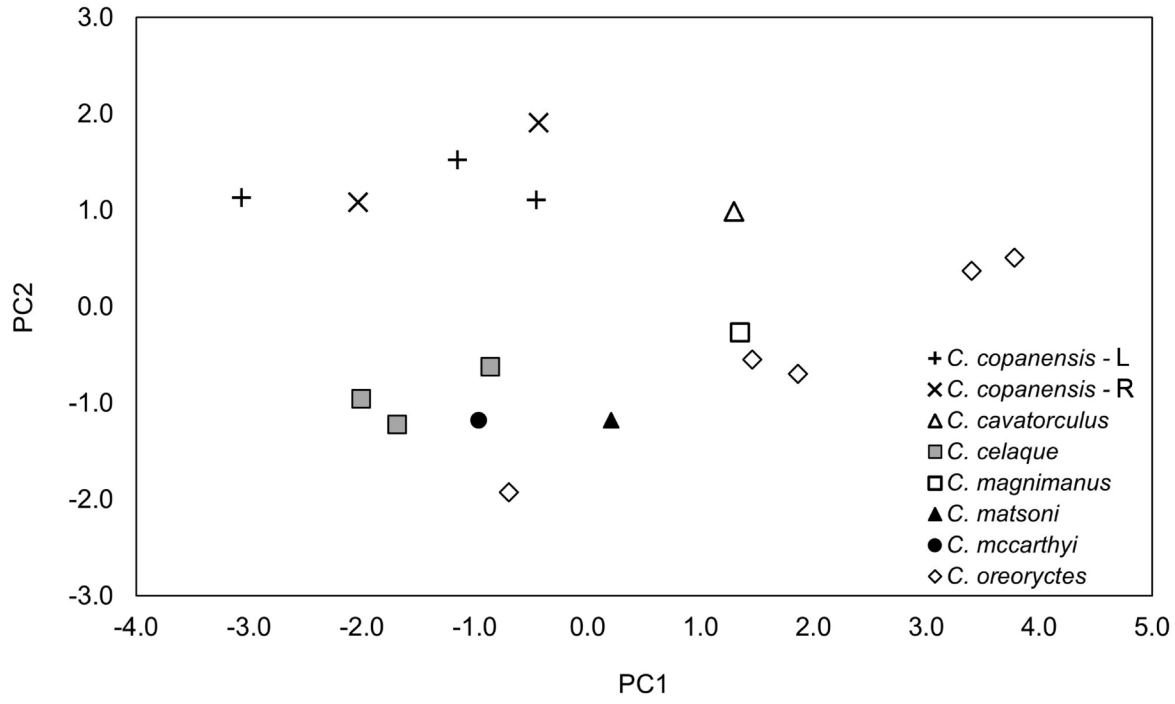

Figure 9. Plots of scores on first two principal components from a PCA of six log10-transformed humerus variables from *C. copanensis* and six species of large-footed *Cryptotis* from Honduras and western Guatemala (see Table 5). Because of the possibility for left (L) and right (R) humeri of *C. copanensis* to have come from the same individual, they are separated in this graph.

DISCUSSION

The *C. goodwini* group is now known to comprise at least 14 species of semi-fossorial shrews that are mostly restricted to high elevation (≥ 1,000 mamsl) moist forests from Chiapas, Mexico, through western Honduras. Relevant genes of most of the species in the group have not yet been sequenced. Species whose genetic sequences have been studied mostly appear to represent relatively shallow divergences that are likely a result of rapid diversification (He et al. 2015, 2021; Baird et al. 2017). In addition, there is evidence for two subclades within the *C. goodwini* group comprised of: 1) species in Guatemala and Chiapas; and 2) Honduran species (He et al. 2015; Baird et al. 2017; Mejía-Fontecha et al. 2021). For this group of shrews—in which closely related species are restricted to scattered, isolated montane regions of limited extent—the topography of southern Mexico and northern Central America represents a sky island complex (McCormack et al. 2009; Love et al. 2023). This pattern is unlike those seen among shrews in the *C. parvus* and *C. nigrescens* clades, which typically occur at lower elevations in the region and have fewer, more widely distributed species (Woodman and Timm 1993; Woodman et al. 2012; Matson and Woodman 2019).

Paleodistribution models for species of *Cryptotis* currently associated with high elevation tropical montane forests in the Sierra Madre Oriental and Sierra Madre del Sur of southern Mexico illustrated how these shrews might have shifted their geographic ranges in response to past climate change (Guevara 2019, 2020). The models indicated that during the cooler and drier conditions of the Last Glacial Maximum (LGM), ca. 26.5–19 ka (Clark et al. 2009), the high-elevation species occurred at lower elevations and occupied considerably broader geographic ranges in moist regions that were latitudinally and longitudinally displaced from their modern distributions. The wider geographic extents of these species provided the potential for larger population sizes, more dispersal among populations, and overall greater genetic connectivity. After the LGM and into the Holocene, these shrews migrated upslope, following cooler, moister conditions favorable for their existence and resulting in smaller, more isolated distributions (Guevara 2019, 2020). Given the number, extent, and duration of climatic fluctuations during the past 2.7 million years (Bintanja et al. 2005; Bintanja and van de Wal 2008; Hughes et al. 2013), the vertical and lateral shifts in distributions indicated by these models—and repeated cycles of independent isolation followed by convergence of populations—likely occurred multiple times, resulting in abundant opportunity for allopatric speciation of isolated populations.

We envision that similar patterns of response to past global climatic fluctuations resulted in the current scattered distribution of species in the *C. goodwini* group across isolated Central American highlands from Chiapas, Mexico, through central Honduras. This makes this group of shrews interesting as a potential model for studies of vicariance and consequences of climate change (Love et al. 2021). Their modern restriction to high elevation habitats of limited extent, however, also renders many of these species, including *C. copanensis* (assuming it is extant), vulnerable to current and future environmental perturbations. In particular, they are at risk of extinction as atmospheric warming increases temperatures and moisture stress in Neotropical high elevation habitats (Pounds et al. 1999; McCain and Colwell 2011; Krishnaswamy et al. 2014; McCain et al. 2021; Love et al. 2023; Corimanya et al. 2025).

ACKNOWLEDGMENTS

We thank the curators and collection managers at Carnegie Museum of Natural History, Pittsburgh; Colección Nacional de Mamíferos, México City; Florida Museum of Natural History, Gainesville; Field Museum of Natural History, Chicago; University of Kansas Natural History Museum and Biodiversity Institute, Lawrence; Museum of Comparative Zoology, Cambridge; The Natural History Museum, London; Senckenberg Naturmuseum, Frankfurt; Museum at Texas Tech University, Lubbock; Museum of Zoology, University of Michigan, Ann Arbor; Universidad Nacional Autónoma de Honduras, Tegucigalpa; Museo

de Historia Natural, Universidad de San Carlos de Guatemala, Guatemala City; National Museum of Natural History, Washington; and Museum Köenig, Bonn, for access to collections and specimens over the years. In particular, we thank William F. Simpson, Adrienne Stroup, and Kenneth D. Angielczyk, Geology Collection, Field Museum, Chicago, for loans and permission to study the materials from Gordon's Cave #3. Eric Sargis and Kristof Zyskowski, Peabody Museum, New Haven, provided facilities in which to study this material. Lisa Bradley and three anonymous reviewers provided substantive input that greatly improved our manuscript.

LITERATURE CITED

Allen JA. 1895. Descriptions of new American mammals. Bulletin of the American Museum of Natural History 7:327–340.

Baird AB, et al. 2017 [2018]. Molecular systematics and biodiversity of the *Cryptotis mexicanus* group (Eulipotyphla: Soricidae): two new species from Honduras supported. Systematics and Biodiversity 16(2):108–117.

Baird SF. 1857. Mammals. In Reports of explorations and surveys, to ascertain the most practicable and economical route for a railroad from the Mississippi River to the Pacific Ocean. Made under the direction of the Secretary of War, in 1853–6, according to acts of Congress of March 3, 1853, May 31, 1854, and August 5, 1854. A. O. P. Nicholson, Printer, Washington, D.C. 8(1):1–757.

Beck J, McCain CM, Brehm G. 2024. Can you trust comparative data based on singleton species? Frontiers of Biogeography 16(1):e62354.

Bintanja R, van de Wal RSW. 2008. North American ice-sheet dynamics and the onset of 100,000-year glacial cycles. Nature 454:869–872.

Bintanja R, van de Wal RSW, Oerlemans J. 2005. Modelled atmospheric temperatures and global sea levels over the past million years. Nature 437:125–128.

Brady JE. 1995. A reassessment of the chronology and function of Gordon's Cave #3, Copán, Honduras. Ancient Mesoamerica 6(1):29–38.

Brady JE. 1996. Retorno a las cavernas de Copán: otra evaluación preliminar. Extraordinario 15:99–118.

Choate JR. 1970. Systematics and zoogeography of Middle American shrews of the genus *Cryptotis*. University of Kansas Publications, Museum of Natural History 19:195–317.

Cifuentes F JE. 2026. Diversidad genética y relaciones filogenéticas de las musarañas de los géneros *Sorex* y *Cryptotis* en Guatemala. Unpublished thesis, Universidad de San Carlos de Guatemala. [https://biblioteca-farmacia.usac.edu.gt/tesis/TB342.pdf; accessed 10 May 2026]

Clark PU, et al. 2009. The Last Glacial Maximum. Science 325(5941):710–714.

Corimanya JL, Jiménez-García D, Li X, Peterson AT. 2025. Geographic patterns of upward shifts in treeline vegetation across western North America, 1984–2017. Biogeosciences 22:5665–5681.

Croft DA. 1998. Micromammal cave fossils from northwestern Honduras. Unpublished master's thesis, University of Chicago, Chicago, Illinois, 29 pp.

Giglioli EH. 1874. Richerche intorno alla distribuzione geografica generale o corologia degli animali vertebrati.Capitolo III. Bollettino della Società Geografica Italiana 11:16–61, 321–345.

Gordon GB. 1898. Caverns of Copán, Honduras. Report on explorations by the museum, 1896–97. Memoirs of the Peabody Museum of Archaeology and Ethnology 1(5):137–148.

Guevara L. 2017. They can dig it: semifossorial habits of the Mexican small-eared shrew (Mammalia: *Cryptotis mexicanus*). Revista Mexicana de Biodiversidad 88:1003–1005.

Guevara L. 2019. Paleodistribution modelling for planning the growth of natural history collections. Revista Mexicana de Biodiversidad 90:e902953.

Guevara L. 2020. Altitudinal, latitudinal and longitudinal responses of cloud forest species to Quaternary glaciations in the northern Neotropics. Biological Journal of the Linnean Society 130:615–625.

Guevara L. 2023. A new species of small-eared shrew (Soricidae: *Cryptotis*) from El Triunfo Biosphere Reserve, Chiapas, Mexico. Journal of Mammalogy 104(3):546–561.

He K, et al. 2021. Mitogenome and comprehensive phylogenetic analyses support rapid diversifications among species groups of small eared shrews genus

Cryptotis (Mammalia: Eulipotyphla: Soricidae). Zoological Research 42(6):739–745.

He K, Chen X, Qiu YB, Liu Z, Wang WZ, Woodman N, et al. 2013. Timing of glaciation during the last glacial cycle: evaluating the concept of a global 'Last Glacial Maximum' (LGM). Earth-Science Reviews 125:171–198.

Hughes PD, Gibbard PL, Ehlers J. 2013. Timing of glaciation during the last glacial cycle: evaluating the concept of a global 'Last Glacial Maximum' (LGM). Earth-Science Reviews 125:171–198.

Hutterer R. 2005. Homology of unicuspids and tooth nomenclature in shrews. Pp. 397–404 in: Merritt JF, Churchfield S, Hutterer R, Sheftel BA, editors, Advances in the biology of shrews II. Special Publication of the International Society of Shrew Biologists 1, New York.

Jackson DA. 1993. Stopping rules in principal components analysis: a comparison of heuristical and statistical approaches. Ecology 74:2204–2214.

Jackson HHT. 1933. Five new shrews of the genus *Cryptotis* from Mexico and Guatemala. Proceedings of the Biological Society of Washington 46:79–81.

Krishnaswamy J, John R, Joseph S. 2014. Consistent response of vegetation dynamics to recent climate change in tropical mountain regions. Global Change Biology 20:203–215.

Linnaeus C. 1766. Systema naturae per regna tria naturae, secundum classes, ordines, genera, species, cum characteribus, differentiis, synonymis, locis. Volume 1. Lurentii Salvii: Stockholm.

Love SJ, Schweitzer JA, Woolbright SA, Bailey JK. 2023. Sky islands are a global tool for predicting the ecological and evolutionary consequences of climate change. Annual Review of Ecology, Evolution, and Systematics 54:219–236.

Lundelius EL, Graham RW, Anderson E, Guilday J, Holman JA, Steadman DW, Webb SD. 1983. Terrestrial vertebrate faunas. Pp. 311–353 in: Porter SC, editor, Late-Quaternary environments of the United States: Vol. 1, the Late Pleistocene, University of Minnesota Press, Minneapolis.

Matson, JO, Woodman N. 2019. Shrews (Eulipotyphla, Soricidae) of Guatemala. Pp. 19–29 in: Kraker C, Calderón AP, Cabrera AA, editors, Perspectivas de investigación sobre los mamíferos silvestres de Guatemala. Asociación Guatemalteca de Mastozoólogos, Ciudad de Guatemala.

Matson, JO, Ordóñez N, Woodman N, Bulmer W, Eckerlin RP, Hanson JD. 2015. Small mammals from the Chelemhá Cloud Forest Reserve, Alta Verapaz, Guatemala. Southwestern Naturalist 59(2014):258–262.

McCain CM, Colwell RK. 2011. Assessing the threat to montane biodiversity from discordant shifts in temperature and precipitation in a changing climate. Ecology Letters 14:1236–1245.

McCain CM, King SRB, TM Szewczyk. 2021. Unusually large upward shifts in cold-adapted, montane mammals as temperature warms. Ecology 102(4):e03300. 10. 1002/ecy. 3300.

McCormack, JE, Huang H, Knowles LL, Gillespie R, Clague D. 2009. Sky islands. Encyclopedia of Islands 4:841–843.

McGrew PO. 1942. Field Museum paleontological expedition to Honduras. Science 96: 85.

McGrew PO. 1944. An *Osteoborus* from Honduras. Geological Series of the Field Museum of Natural History 8:75–77.

Meachen J A, Samuels JX. 2012. Evolution of coyotes (*Canis latrans*) in response to the megafaunal extinctions. Proceedings of the National Academy of Sciences 109(11):4191–4196.

Mejía-Fontecha IY, Velásquez-Guarín D, Tapie KDP, Ossa-López PA, Rivera-Páez FA, Ramírez-Chaves HE. 2021. First record of the northern Ecuadorian shrew, *Cryptotis niausa* Moreno Cárdenas and Albuja, 2014 (Eulipotyphla, Soricidae), in Colombia. Check List 17(5):1345–1352.

Merriam CH. 1895. Revision of the American genera *Blarina* and *Notiosorex*. North American Fauna, 10:5–34, pls. 1–3.

Merriam CH. 1901. Seven new mammals from Mexico, including a new genus of rodents. Proceedings of the Washington Academy of Science 3:559–563.

Millien V, Lyons SK, Olson LE, Smith FA, Wilson AB, Yom-Tov Y. 2003. Ecotypic variation in the context of global climate change: revisiting the rules. Ecology Letters 9:853–869.

Moreno Cárdenas PA. 2017. Sistemática y biogeografía de las musarañas del género *Cryptotis* (Eulipotyphla: Soricidae) en los Andes de Ecuador. Unpublished M.S. thesis, Pontificia Universidad Católica del Ecuador, Quito.

Ochocińska D, Taylor JRE. 2003. Bergmann's rule in shrews: geographical variation of body size in Palearctic

Sorex species. Biological Journal of the Linnean Society 78:365–381.

Olson E, McGrew PO. 1942. Mammalian fauna from the Pliocene of Honduras. Bulletin of the Geological Society of America 52:1219–1244.

Ordóñez-Garza NJ, Matson O, Eckerlin RP, Bulmer W, Greiman SE. 2014. Small mammal community from an isolated, remnant cloud forest in Guatemala. Occasional Papers, Museum of Texas Tech University 324:1–7.

Pomel A. 1848. Etudes sur les carnassiers insectivores (Extrait). Seconde partie.—Classification des insectivores. Archives des Sciences Physiques et Naturelles, Genève 9:244–251.

Pounds JA, Fogden MPL, Campbell JH. 1999. Biological response to climate change on a tropical mountain. Nature 398:611–615.

Rue DJ, Freter AC, Ballinger DA. 1989. The caverns of Copán revisited: Preclassic sites in the Sesesmil River Valley, Copán, Honduras. Journal of Field Archaeology 16(4):395–404.

Say T, Ord G. 1825. Description of a new species of Mammalia, whereon a genus is proposed to be founded. Journal of the Academy of Natural Sciences of Philadelphia 4(2):352–355 + pl. 22.

Stehli FG, Webb SD (eds.). 1985. The Great American Biotic Interchange. Topics in geobiology. New York: Plenum Press.

Stuiver M, Reimer PJ. 1993. Extended ^{14}C data base and revised CALIB 3.0 ^{14}C age calibration program. Radiocarbon 35(1):215–230. (http://calib.org/calib/)

Woodman N. 2005. Size evolution in Goodwin's small-eared shrew, *Cryptotis goodwini*. Pp. 125–138 in: Merritt JF, Churchfield S, Hutterer R, Sheftel BA, editors, Advances in the biology of shrews II. Special Publication of the International Society of Shrew Biologists 1, New York.

Woodman N. 2010. Two new species of shrews (Soricidae) from the western highlands of Guatemala. Journal of Mammalogy 91(3):566–579.

Woodman N. 2011. Patterns of morphological variation amongst semifossorial shrews in the highlands of Guatemala, with the description of a new species (Mammalia, Soricomorpha, Soricidae). Zoological Journal of the Linnean Society 163:1267–1288.

Woodman N. 2015. Morphological variation among broad-clawed shrews (Mammalia: Eulipotyphla: Soricidae: *Cryptotis* Pomel, 1848) from highlands of western Honduras, with descriptions of three new cryptic species. Annals of Carnegie Museum 83(2):95–119.

Woodman N. 2018. American Recent Eulipotyphla: nesophontids, solenodons, moles, and shrews in the New World. Smithsonian Contributions to Zoology 650:i–vi, 1–109.

Woodman N. 2019. Three new species of small-eared shrews, genus *Cryptotis*, from El Salvador, Guatemala, and Honduras (Mammalia: Eulipotyphla: Soricidae). Special Publications, Museum of Texas Tech University 72:1–46.

Woodman N, Croft DA. 2005. Fossil shrews from Honduras and their significance for late Glacial evolution in body size (Mammalia: Soricidae: *Cryptotis*). Fieldiana, Geology, new series 51:i–iv, 1–30.

Woodman N, Gaffney SA. 2014. Can they dig it? Functional morphology and semifossoriality among small-eared shrews, genus *Cryptotis* (Mammalia, Soricidae). Journal of Morphology 275:745–759.

Woodman N, Stabile FA. 2015. Functional skeletal morphology and its implications for locomotory behavior among three genera of mysoricine shrews (Eulipotyphla: Soricidae). Journal of Morphology 276:550–563.

Woodman N, Timm RM. 1992. A new species of small-eared shrew, genus *Cryptotis* (Insectivora: Soricidae), from Honduras. Proceedings of the Biological Society of Washington 105:1–12.

Woodman N, Timm RM. 1993. Intraspecific and interspecific variation in the *Cryptotis nigrescens* species complex of small-eared shrews (Insectivora: Soricidae), with the description of a new species from Colombia. Fieldiana: Zoology (new series) 74:1–30.

Woodman N, Timm RM. 1999. Geographic variation and evolutionary relationships among broad-clawed shrews of the *Cryptotis goldmani*-group (Mammalia: Insectivora: Soricidae). Fieldiana: Zoology (new series) 91:1–35.

Woodman N, Wilken AT. 2019. Comparative functional skeletal morphology among three genera of shrews: implications for the evolution of locomotory behavior in the Soricinae (Eulipotyphla: Soricidae). Journal of Mammalogy 100(6):1750–1764.

Woodman N, Matson JO, McCarthy TJ, Eckerlin RP, Bulmer W, Ordóñez-Garza N. 2012. Distributional records of shrews (Mammalia, Soricomorpha) from northern Central America, with the first record of *Sorex* from Honduras. Annals of the Carnegie Museum 80(3):207–237.

Yom-Tov Y, Yom-Tov J. 2005. Global warming, Bergmann's rule and body size in the masked shrew *Sorex cinereus* Kerr in Alaska. Journal of Animal Ecology 74(5):803–808.

Addresses of authors:

NEAL WOODMAN

148 Fleetwood Terrace
Silver Spring, MD 20910
nlwdman@gmail.com

DARIN A. CROFT

Department of Anatomy
Case Western Reserve University
School of Medicine
10900 Euclid Avenue
Cleveland, Ohio 44106-4930
dac34@case.edu

This submission was handled by Subject Editor Jeffrey W. Martz.

APPENDIX

Specimens from the following institutions were used in this study for comparison and measurements. Institutional abbreviations follow Dunnum et al. (2018:supplementary data SD4): Carnegie Museum of Natural History, Pittsburgh (CM); Colección Nacional de Mamíferos, Instituto de Biología, Universidad Nacional Autónoma de México, México City (CNMA); Florida Museum of Natural History, Gainesville (FLMNH); Field Museum of Natural History, Chicago (FMNH); University of Kansas Natural History Museum and Biodiversity Institute, Lawrence (KU); Museum of Comparative Zoology, Cambridge (MCZ); The Natural History Museum, London (NHM); Senckenberg Naturmuseum, Frankfurt (SMF); Museum at Texas Tech University, Lubbock (TTU); Museum of Zoology, University of Michigan, Ann Arbor (UMMZ); Universidad Nacional Autónoma de Honduras, Tegucigalpa (UNAH); Museo de Historia Natural, Universidad de San Carlos de Guatemala, Guatemala City (USAC); National Museum of Natural History, Washington (USNM); and Museum Köenig, Bonn (ZMFK).

Dentaries

Cryptotis cavatorculus (*n* = 1).—HONDURAS: Santa Barbara: Parque Nacional de Santa Barbara, desiccated cloud forest on a ridge above El Cedral, ca. 1,900 m (FLMNH 27718—holotype).

Cryptotis celaque (*n* = 13).—HONDURAS: Lempira: Celaque National Park: Visitors Center, 1,430 m (CM 118519); Campamento Don Tomás, 2,075 m (CM 112878, 112879, 112880, 112881, 112882—holotype); Campamento Naranjo, 2,560 m (CM 119710, 119711, 119712, 119713, 119714, 119715, 119716; 1 uncatalogued UNAH).

Cryptotis eckerlini (*n* = 8).—GUATEMALA: Sacatepéquez: Cerro Cucurucho; 11 km by road SE of Antigua Guatemala; Finca El Pilar (14º 31.112' N, 90º 41.472' W); 2,640 m (TTU 136183, 136184, 136185, 136186, 136187, 136188, 136189, 136192).

Cryptotis goodwini (*n* = 32).—GUATEMALA: Quetzaltenango: Calel, 10,200 ft (USNM 77070, 77072, 77073, 77074—holotype, 77075, 77076, 77077, 77078, 77079, 77080, 77081, 77082, 77083, 77084); Volcán Santa María, 9,000–11,000 ft (USNM 77086, 77087). San Marcos: Finca La Paz, 1,200 m (UMMZ 103416). San Marcos: S slope Volcán Tajumulco, 10,000 ft (UMMZ 99541). Baja Verapaz: 5 mi N, 1 mi W El Chol, 6,000 ft (KU 64611). Chimaltenango: Santa Elena, 9,900–10,000 ft (FMNH 41791, 41792, 41793, 41794); Tecpán, 9,700 ft (AMNH 74302). Totonicapan: Cumbre María Tecún, 3,000 m (UMMZ 112004, 112005, 112006, 112007, 112008, 112009, 112010, 112011).

Cryptotis griseoventris (*n* = 10).—MEXICO: Chiapas: San Cristóbal de las Casas, 8,000–9,500 feet (USNM 75886, 75887, 75888, 75889, 75891, 75892, 78594); 6 mi SE San Cristobal de las Casas (MCZ B48061).

Cryptotis lacertosus (*n* = 8).—GUATEMALA: Huehuetenango: 5 km SW San Mateo Ixtatán, 3,110 m (USNM 569420, 569431, 569442, 569443, 569503); Yaiquich [ca. 15º 45' 44" N, 91º 30' 10" W], 2,680 m (USNM 569368); San Mateo Ixtatán, ca. 4 km NW Santa Eulalia, Yaiquich, 2,950 m (UMMZ 117843); 3.5 mi SW San Juan Ixcoy, 10,120 ft (KU 64610).

Cryptotis magnimanus (*n* = 1).—HONDURAS: Comayagua: 2.5 km N, 1.6 km E Cerro San Juanillo, Reserva Biológica Cordillera de Montecillos, 1,730 m (KU 144611—holotype).

Cryptotis mam (*n* = 28).—GUATEMALA: Huehuetenango: Todos Santos Cuchumatán, 10,000 ft (USNM 77051, 77052, 77053, 77054, 77055, 77056, 77057, 77058, 77059, 77060, 77061, 77062, 77063, 77064, 77065, 77066, 77067, 77068); Hacienda Chancol, 9,500–11,000 ft (USNM 77069); Laguna Magdalena, 2,925 m (USNM 569554, 569555, 570337, 570340); Puerto al Cielo, 3,350 m (USNM 570248); Aldea El Rancho, 3,020 m (USNM 570256, 570257, 570313, 570314).

Cryptotis matsoni (*n* = 1).—GUATEMALA: Jalapa: 11.6 km east of Mataquescuintla, 2,560 m (USNM 275681—holotype).

Cryptotis mccarthyi (*n* = 17).—HONDURAS: Cortés: Cusuco National Park, ca. 0.3 km SW of the Visitors Center, 1,500–1,600 m; ca. 15º30' N, 88º13' W (CM 119693—holotype, 119694, 119695, 119696, 119697, 119698, 119699, 119700, 119701, 119702, 119703, 119704, 119705, 119706, 119707, 119708, 119709).

Cryptotis montecristo (*n* = 1).—EL SALVADOR: Santa Ana: Hacienda Montecristo, north of Metapán; in cloud forest at 2,150 m (SMF 14837—holotype).

Cryptotis oreoryctes (*n* = 13).—GUATEMALA: Alta Verapaz: Chelemhá, 2,090 m (CM 120097, 120100, 120102; USNM 569854, 569877, 569878); Chinaux, 2,042 m (CM 120103, 120104, 120105, 120106); Cobán (NHM 7.1.1.35, NHM 43.9.15.5). El Progreso: Cerro Pinalón, Camino a las Torres, 2,700 m (CM 113275). Zacapa: 6 km NNW of San Lorenzo, 2,200 m, ca. 15.5 km NNW of Río Hondo (CM 113276; USAC no number [SGP 500]).

Cryptotis woodmani (*n* = 2).—MEXICO: Chiapas: 17 km SE Finca Prusia (CNMA 22784); Catarina, 1,300 m (ZFMK 63.484).

Humeri

Cryptotis cavatorculus (*n* = 1).—FLMNH 27718.

Cryptotis celaque (*n* = 3).—CM 112880, 112882; 1 uncatalogued UNAH.

Cryptotis magnimanus (*n* = 1).—KU 144611.

Cryptotis matsoni (*n* = 1).—USNM 275681.

Cryptotis mccarthyi (*n* = 1).—CM 119697.

Publications of the Museum at Texas Tech University

Institutional subscriptions to Occasional Papers are available through the Museum of Texas Tech University, attn: NSRL Publications Secretary, Box 43191, Lubbock, TX 79409-3191. Individuals may also purchase separate numbers of the Occasional Papers directly from the Museum at Texas Tech University.

Series Editor: Caleb D. Phillips
Production Editor: Lisa Bradley

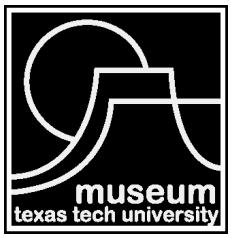

ISSN 0149-175X (print)

ISSN 3143-4150 (online)

Museum at Texas Tech University, Lubbock, TX 79409-3191